ISSN 1674-1056
http://cpb.iphy.ac.cn
http://iopscience.iop.org/cpb
中国物理 B
Chinese Physics
中国物理
Chinese Physics B

Simulation and experiment investigation of low frequency vibration reduction of honeycomb phononic crystal

Han-Bo Shao(邵瀚波), Guo-Ping Chen(陈国平), Huan He(何欢), Jin-Hui Jiang(姜金辉)

Citation: Chin. Phys. B . 2018, 27(12): 126301. **doi:** 10.1088/1674-1056/27/12/126301
Journal homepage: http://cpb.iphy.ac.cn; http://iopscience.iop.org/cpb

What follows is a list of articles you may be interested in

Power flow analysis in a hybrid phononic crystal structure

Hanbei Guo(郭寒贝), Qiang Li(李强), Liubin Zhou(周刘彬), Lei Qiang(强磊)

Chin. Phys. B . 2018, 27(3): 036302. **doi:** 10.1088/1674-1056/27/3/036302

Bismuth-content-dependent polarized Raman spectrum of InPBi alloy

Guan-Nan Wei(魏冠男), Qing-Hai Tan(谭青海), Xing Dai(戴兴), Qi Feng(冯琦), Wen-Gang Luo(骆文刚), Yu Sheng(盛宇), Kai Wang(王凯), Wen-Wu Pan(潘文武), Li-Yao Zhang(张立瑶), Shu-Min Wang(王庶民), Kai-You Wang(王开友)

Chin. Phys. B . 2016, 25(6): 066301. **doi:** 10.1088/1674-1056/25/6/066301

Complete low-frequency bandgap in a two-dimensional phononic crystal with spindle-shaped inclusions

Ting Wang(王婷), Hui Wang(王辉), Mei-Ping Sheng(盛美萍), Qing-Hua Qin(秦庆华)

Chin. Phys. B . 2016, 25(4): 046301. **doi:** 10.1088/1674-1056/25/4/046301

Study on lattice vibrational properties and Raman spectra of Bi_2Te_3 based on density-functional perturbation theory

Feng Song-Ke, Li Shuang-Ming, Fu Heng-Zhi

Chin. Phys. B . 2014, 23(8): 086301. **doi:** 10.1088/1674-1056/23/8/086301

Tuning of band-gap of phononic crystals with initial confining pressure

Feng Rong-Xin, Liu Kai-Xin

Chin. Phys. B . 2012, 21(12): 126301. **doi:** 10.1088/1674-1056/21/12/126301

Simulation and experimental investigation of low-frequency vibration reduction of honeycomb phononic crystals*

Han-Bo Shao(邵瀚波), Guo-Ping Chen(陈国平)†, Huan He(何欢), and Jin-Hui Jiang(姜金辉)

State Key Laboratory of Mechanics and Control of Mechanical Structures, College of Aerospace Engineering, Nanjing University of Aeronautics and Astronautics, Nanjing 210016, *China*

(Received 8 August 2018; revised manuscript received 27 September 2018; published online 10 November 2018)

The honeycomb phononic crystal displays good performance in reducing vibration, especially at low frequency, but there are few corresponding experiments involving this kind of phononic crystal and the influence of geometric parameters on the bandgap is unclear. We design a honeycomb phononic crystal, which is assembled by using a chemigum plate and a steel column, calculate the bandgaps of the phononic crystal, and analyze the vibration modes. In the experiment, we attach a same-sized rubber plate and a phononic crystal to a steel plate separately in order to compare their vibration reduction performances. We use 8×8 unit cells as a complete phononic crystal plate to imitate an infinite period structure and choose a string suspension arrangement to support the experiment. The results show that the honeycomb phononic crystal can reduce the vibrating plate magnitude by up to 60 dB in a frequency range of 600 Hz–900 Hz, while the rubber plate can reduce only about 20 dB. In addition, we study the effect of the thickness of plate and the height and the radius of the column in order to choose the most superior parameters to achieve low frequency and wide bandgap.

Keywords: honeycomb phononic crystal, reducing vibration, bandgap

PACS: 63.20.–e, 63.20.D– **DOI:** 10.1088/1674-1056/27/12/126301

1. Introduction

In modern warfare, military aircraft[1–3] play an indispensable role. How to reduce low-frequency vibration from our own equipment or enemy attack is key to measuring the combat performance of the aircraft. However, it is difficult to control the vibration of aircraft from the source because of many complicated reasons.[4–7] So, designing a kind of material with a low-frequency vibration reducing characteristic is very important.

Because there are many limitations to the practical engineering applications of traditional materials, artificial composite materials with special physical properties have become the focus of attention.[8] Phononic crystal[9–12] is a composite material composed of two or more materials with different bandgaps, and its elastic constant, density and sound velocity always change periodically. Phononic crystal has many good physics characteristics, of which the most significant and attractive is that it can reduce vibration and noise when the frequency of the elastic wave is at the bandgap frequency;[13] thus, the lower bandgap can be obtained by selecting a suitable scatterer, substrate and cladding layer, which can be used for controlling low-frequency vibration in mechanical equipment.

The formation of bandgaps is attributed to Bragg scattering[14,15] or the local resonance.[16] When the initial frequency of a bandgap is equal, the lattice constant of the local resonance phonon crystal is 1–2 orders of magnitude smaller than that of Bragg scattering type, which is suitable for controlling medium and low frequency noise.[17] The idea of local resonance phononic crystal was first described by Liu *et al.* in 2000;[18] then, a new field of phononic crystals opened up. There have been many studies of local resonance phonon crystals over the past two decades, mainly in the field of bandgap formation mechanism and bandgap calculation method or passive and active control of bandgap width and position. Wen *et al.*[13] introduced the bandgap mechanism and characteristics about Bragg scattering and the local resonance phononic crystal; moreover, they proposed five methods to calculate the bandgaps and studied two-dimensional (2D) phononic crystal with a honeycomb structure. They chose steel as the scatterer and chemigum as the base; analyzing and calculating the band structure with a concentrated mass method and obtaining a bandgap range from 200 Hz to 270 Hz. Zhang *et al.*[19] came up with a new hybrid phononic crystal and studied the effects of the geometrical parameters to control the wave propagation. They used the finite element method to calculate the bandgaps, successfully obtaining a wide gap between 247.996 Hz and 979.1 Hz. Li *et al.*[20] realized the active controlling of the bandgap of an elastic beam by using piezoelectric sensors with periodic distribution. They placed piezoelectric actuators and piezoelectric sensors above and below the beam, respectively, and adjusted the position and width of the bandgap through changing the parameters of the piezoelectric material and external control voltages. They designed a negative proportional feedback control method that adds an active stiffness to the elastic beam and is more flexible than passive control, which

*Project supported by the Fundamental Research Funds for the Central Universities, China (Grant No. NS2017003).

†Corresponding author. E-mail: gpchen@nuaa.edu.cn

© 2018 Chinese Physical Society and IOP Publishing Ltd

focuses on changing the parameters of the phononic crystal themselves.

However, most of the experiments on phononic crystal for reducing the low-frequency vibration focus on the bandgap of the crystal itself. There are few experiments on reducing the vibrations of real objects and there are fewer comparative experiments involving the honeycomb phononic crystal at low frequency. So, although many simulations show that the phononic crystal can reduce vibration in their bandgap, it is less persuasive than a concrete experiment. Sun[21] designed an experiment on an acoustic metamaterial, which had physical properties similar to those of phononic crystal and successfully verified that the metamaterial could reduce the vibrating plate resonance magnitudes by up to 42 dB in its system. In this paper, we design a honeycomb phononic crystal assembled by using a chemigum plate and a steel column, analyze its bandgap and transmission characteristics, and we attach a same-sized rubber plate and phononic crystal separately to a steel plate in order to make a comparison between their vibration reduction performances. We performed the simulation and its corresponding experiment to verify the physical properties in reducing vibration. We notice that this phononic crystal has a bandgap ranging from nearly 600 Hz to 900 Hz, and it can reduce vibration by up to 60 dB (averaging 23.32 dB). We also study the effect of the thickness of plate and the height and the radius of the column in order to choose the most superior parameter to achieve a low frequency and wide bandgap.

This paper aims to verify the vibration reduction characteristics experimentally and designs a most superior structure by optimizing the geometric parameters of the structure for reducing the low-frequency vibration. The present study provides new ideas and methods for practical application and has profound implications for military aircraft and related research.

2. Models and theoretical calculation

Phononic crystal is a periodic composite, and its structure has elastic wave bandgaps, yet infinite periodic phononic crystal is only an ideal model. In the real world, phononic crystal only has a finite period, so we can simplify it into an original cell with periodic boundary conditions according to the band theory. The elastic wave propagation characteristics are reflected by the energy band structure, and the bandgap characteristics are described by the transmission characteristics of the incident elastic wave.

Phononic crystal has a honeycomb structure, which is assembled by using a chemigum plate and steel column. We use 8×8 unit cells as a complete phononic crystal plate to imitate an infinite period structure, the unit cell and the complete phononic crystal plate are shown in Fig. 1. The diamond side length of the chemigum plate is $a = 0.036$ m, (a is also the lattice constant) and the radius of the steel column is $r = 0.008$ m. The thickness of the plate and the height of the column are $t = 0.003$ m and $h = 0.018$ mm, respectively. All the material properties are listed in Table 1.

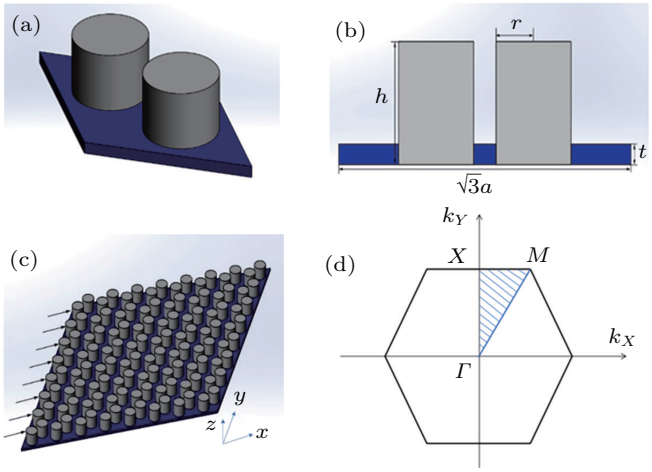


Fig. 1. (color online) Phononic crystal model diagram, showing (a) unit cell diagram, (b) cross section diagram of a unit cell, (c) complete phononic crystal plate, and (d) corresponding first irreducible Brillouin zone (shaded region).

Table 1. Material properties of the honeycomb plate.

Component	Young's modulus/GPa	Poisson's ratio	Density/(kg/m^3)
Inclusion of core (steel)	200.6	0.3	7780
Triangular lattice plate (chemigum)	0.0054	0.5	1300

We calculate the bandgaps of the phononic crystal by using the finite element method (FEM). The unit cell is meshed and divided into finite elements. We can use the following generalized elastic eigenvalue to solve the problem, which can be written as

$$\left(\boldsymbol{K} - \omega^2 \boldsymbol{M}\right) \boldsymbol{U} = \boldsymbol{0}, \tag{1}$$

where $\boldsymbol{K}$ and $\boldsymbol{M}$ are the stiffness and mass matrix, respectively. $\boldsymbol{U} = [\boldsymbol{U}_1 \ \boldsymbol{U}2 \ \cdots \ \boldsymbol{U}_{\mathrm{n}}]^{\mathrm{T}}$ is the displacement matrix of the unit cell and $\boldsymbol{U}_i = \left[u_i \ v_i \ w_i \right]^{\mathrm{T}}$ are the displacements at the nodes of the elements. Based on the Bloch theorem, the displacement vector $\boldsymbol{u}(\boldsymbol{r})$ has the form

$$\boldsymbol{u}(\boldsymbol{r}) = \boldsymbol{u}_k(\boldsymbol{r})\, \mathrm{e}^{(\mathrm{i}\boldsymbol{k}\cdot\boldsymbol{r})}, \tag{2}$$

where the wave vector $\boldsymbol{k} = (k_x, k_y)$ is confined in the first Brillouin zone of the unit cell, and $\boldsymbol{r} = (x, y, z)$ and $\boldsymbol{u}_k(\boldsymbol{r})$

are the position vector and a periodical vectorial function, respectively. Periodic boundary conditions can be obtained by Eq. (2) based on the Bloch theorem

$$\boldsymbol{U}(\boldsymbol{r}+\boldsymbol{a}) = \boldsymbol{U}(\boldsymbol{r})\,\mathrm{e}^{(\mathrm{i}\boldsymbol{k}\cdot\boldsymbol{a})}, \tag{3}$$

where $\boldsymbol{a}$ is the lattice constant of the unit cell.

We take the wave vector k all over the boundary of the Brillouin region. M, X, and Γ are three of the vertices. Thus, the band structure can be calculated as shown in Fig. 2. From the figure we can observe that the first wider bandgap is located in a range of 600 Hz–900 Hz, which shows that elastic wave propagation is inhibited in this frequency range, yet it can be propagated in another frequency range without any loss. There are also many very thin bandgaps, just like the bandgap between 1100 Hz and 1500 Hz. Owing to the fact that the bandgap is very narrow, and it is not very useful in practical applications, we do not take it into consideration. The vibration modes are depicted in Fig. 3, it is easy to see that the lower edge of the bandgap (586.58 Hz) is present as the bending vibration appears at the obtuse apex of the diamond plate and the vertical vibration occurs at the acute apex. However, the upper edge of the bandgap (893.46 Hz) presents as the vertical vibration at the obtuse apex while little vibration occurs at the acute apex. It is the vibration difference that leads to the generation of the bandgap.

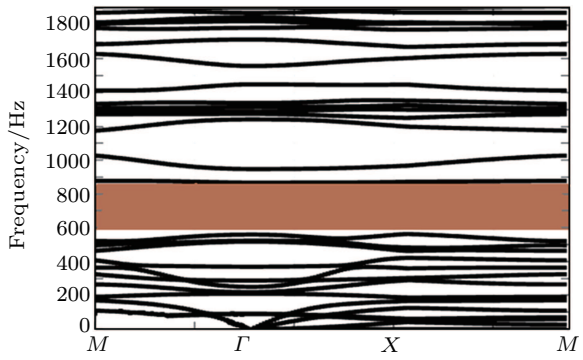


Fig. 2. (color online) Bandgap of phononic crystal.

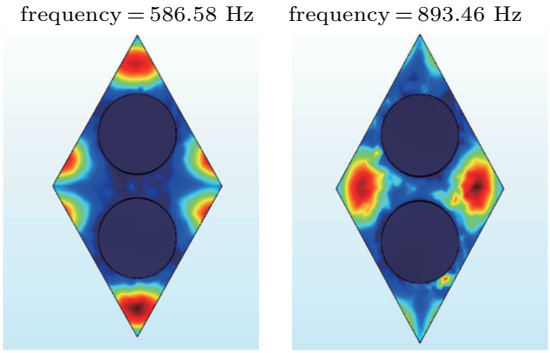


Fig. 3. (color online) Vibration modes of phononic crystal, showing (a) lower edge of the bandgap, and (b) upper edge of the bandgap.

Moreover, we do not consider the physics character in the z direction because the periodicity only exists in the x- and y-directions, and we use only the acceleration in one of the directions in the x–y plane because of the symmetry. An acceleration of '1' is applied to the left boundary in Fig. 1(c); its direction is perpendicular to the edge of the boundary and the remaining boundaries are free boundaries. We also calculate the transmission characteristic of the phononic crystal by using the software Comsol for comparisons with the bandgap. The transfer characteristic equation is defined as

$$H = 10\log\left(\frac{\int_{S_1}|a_1|\,\mathrm{d}S_1}{\int_{S_2}|a_2|\,\mathrm{d}S_2}\right), \tag{4}$$

where a_1 and a_2 are the acceleration of the transmitted and incident boundary, respectively. S_1 and S_2 are the area of the transmitted and the incident boundary, respectively. The transmission characteristic is shown in Fig. 4. We can notice that the response from the output terminal decreases sharply in a range of shadows (586.58 Hz–893.46 Hz), indicating that the vibration is attenuated obviously in this frequency range. Thus, the effect of vibration reduction can be verified by comparing with the bandgap in Fig. 2.

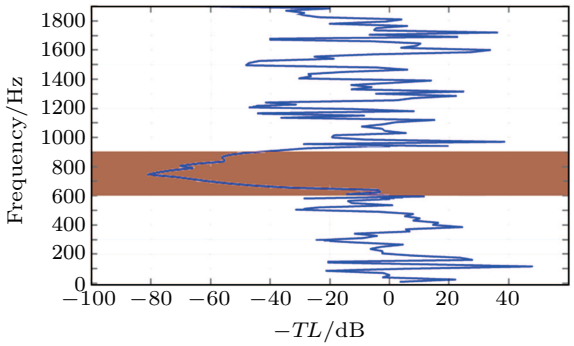


Fig. 4. (color online) Transmission characteristic of phononic crystal.

In this section, we verify that this honeycomb phononic crystal has a bandgap ranging from 586.58 Hz to 893.46 Hz, which can reduce vibration and prevent wave propagation. In the following section, we will further verify its vibration damping characteristics through simulation and experiment.

3. Simulation

To verify the vibration damping characteristics of this honeycomb structure more practically, we attach the phononic crystal to a steel plate (Fig. 5(a)) and measure its frequency response curve. mMoreover, a chemigum plate without holes is also attached to a steel plate (Fig. 5(b)) and its frequency response curve is measured so that we can compare the two cases.

Two incentive points and two response points are selected in the steel plate, as shown in Fig. 6. We apply 1 N to each of the two incentive points and can obtain two groups of data for each inventive point. It is easy to notice in the frequency response function from Fig. 7, whether it is a solid line or a dash

line (response at point one or point two), the response relatively declines when the steel plate is attached to the phononic crystal in a frequency range from 600 Hz to 900 Hz. Conversely, there is little difference between the naked steel plate and the steel + rubber plate, which verifies that the phononic crystal with this honeycomb structure can provide a good vibration damping performance in its bandgap. The result is also consistent with the transmission diagram, which is shown in the previous section.

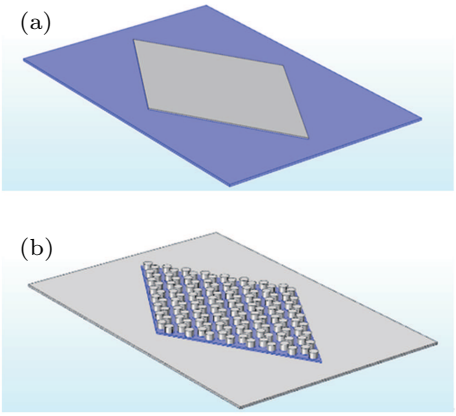


Fig. 5. (color online) Models of simulation for (a) rubber-attached crystal and (b) phononic-attached crystal.

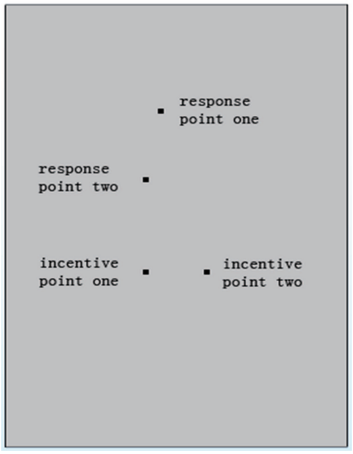


Fig. 6. Incentive and response points.

To show the vibration damping characteristics more clearly, we define two variables below.

$$\Delta H_{\text{rub}} = H_{\text{rub}} - H_{\text{steel}},$$
$$\Delta H_{\text{pho}} = H_{\text{pho}} - H_{\text{steel}}, \tag{5}$$

where H_{rub}, H_{steel}, and H_{pho} are the values of the frequency response function (FRF) when the frequency ranges from 600 Hz to 900 Hz. The difference between the rubber and phononic crystal is displayed in Fig. 8, where the red line and green line represent the vibration reduction amplitude of phononic crystal and rubber, respectively. We can also easily notice from Figs. 8(a) and 8(b) that the red line is lower than the green line at each frequency, no matter if it is solid line or dash line, showing that the phononic crystal has better vibration reduction performance than rubber. When the incentive is at point one, the phononic crystal plate can reduce the vibration magnitude by more than 40 dB at response point one, and by nearly 60 dB at response point two (averaging 19.86 Hz and 23.32 Hz at response point one and two, respectively). Similarly, when the incentive is at point two, the vibration magnitude is also reduced by up to 40 dB (averaging 20.14 Hz

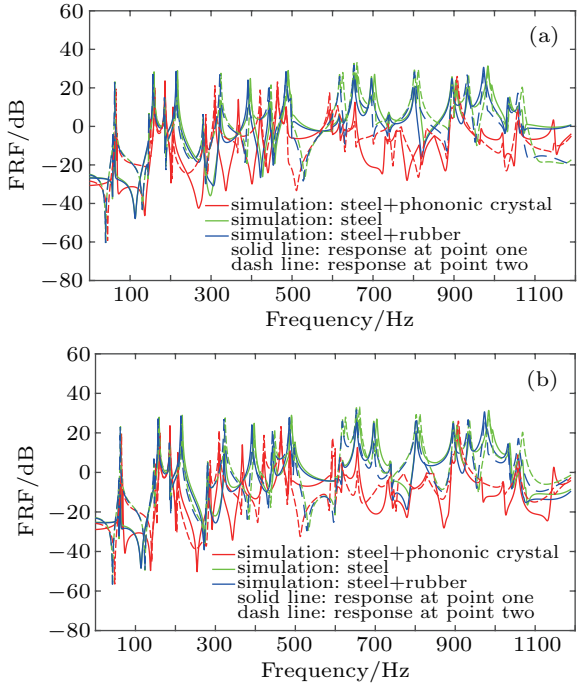


Fig. 7. (color online) Frequency response function for (a) incentive at point one, (b) incentive at point two.

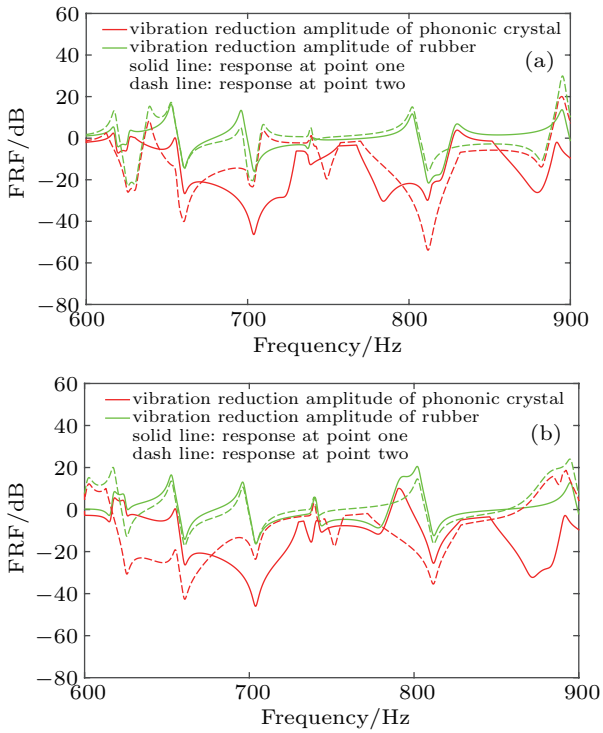


Fig. 8. (color online) Vibration magnitude reduction for (a) incentive at point one and (b) incentive at point two.

and 17.36 Hz at response point one and two respectively), however, the maximum vibration magnitude reduction of rubber is only 20 dB, which further shows that the phononic crystal plate has a better vibration reduction performance.

4. Experimental results

We perform a corresponding experiment to verify the simulation results. The materials used in the experiment are shown in Fig. 9. The geometric parameters and physical parameters are the same as those in the simulation, which is indicated in Table 1 and Fig. 1. In addition, a string suspension arrangement is chosen (Fig. 10) to support the experimental workpiece because it provides the least damping effect and nearly free boundary conditions. Point A and point B represent the two positions of two incentives. We use an impact hammer (model: PCB 086C02) to provide the excitation. Moreover, the acceleration response the signals of the plate at different points that are sampled by using two accelerometers (model: PCB 356A26), frequency response function of the plate structure is recorded by the Vibmobike signal collection analyzer (software is m+p smartoffice). The incentive points and response points are shown in Fig. 6.

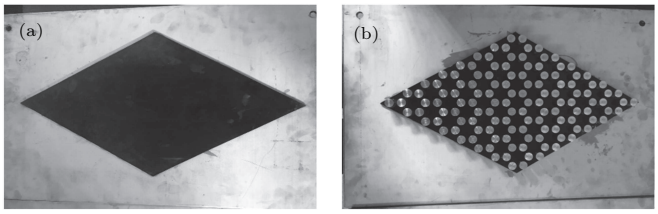


Fig. 9. Materials used in experiment, showing (a) rubber- and (b) phononic-crystal-attached steel plates.

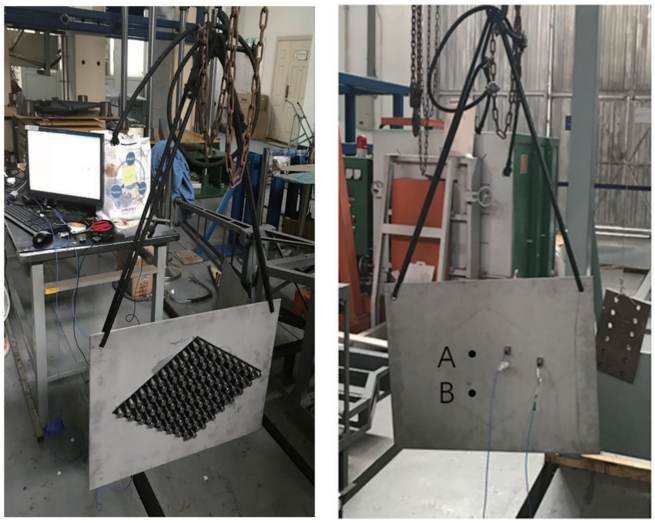


Fig. 10. (color online) String suspension arrangement.

The experimental results are then organized and processed by Matlab software, which are shown in Fig. 11. Figures 11(a) and 11(b) show the incentive at point one and the incentive at point two, respectively.

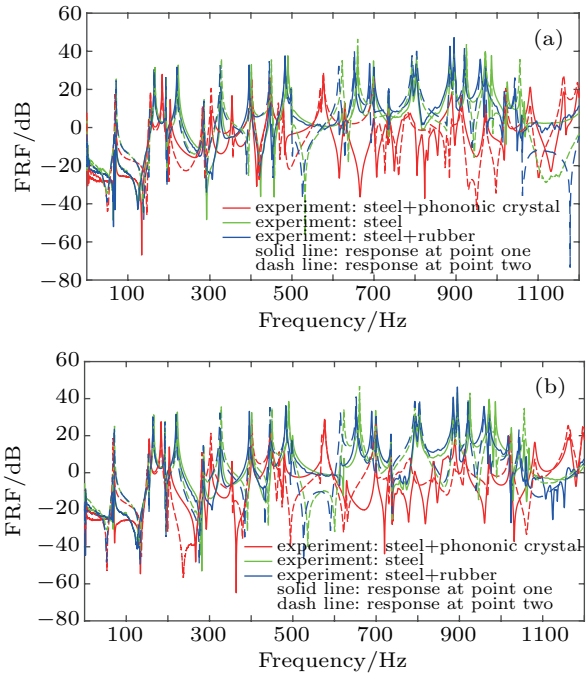


Fig. 11. (color online) Vibration magnitude reduction for (a) incentive at point one and (b) incentive at point two.

We can notice that the results are the same as simulation: the vibration decreases more sharply for phononic crystal than for rubber in a frequency range from 600 Hz to 900 Hz (in the bandgap), and the magnitude decreases by up to near 60 dB (averaging 20.36 Hz, 26.12 Hz, 23.96 Hz, and 19.19 Hz at response points one and two, respectively). The average values are slightly larger than the simulation values, for which the main reason is that we do not consider the effect of damping in the simulation and there are some losses of energy in the experiment. So, the vibration reduction performance of phononic crystal in the practical application is inferior to that of simulation.

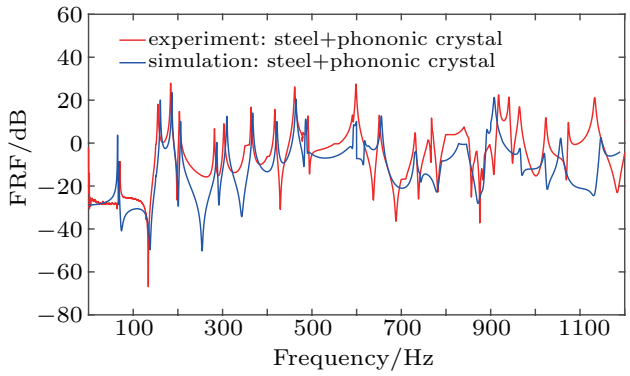


Fig. 12. (color online) Comparison between experimental results and simulation results.

Figure 12 shows the comparison between the experimental results and the simulation results. We consider the case that the incentive is at point one and the response is also at point one. We can find that, before 900 Hz, the experimental results accord well with the simulation results, especially at the peaks

of the curve, while the values at the valley point present little errors at some frequencies, which most likely is due to the effect of damping in the preparation of materials. The error is slightly larger after 900 Hz, the reason is that when we use a force-hammer to make an incentive, the energy concentrates at low frequencies and we cannot collect the signals of high frequency very well, so the error will become larger with the increase of the frequency.

5. Parameter effect on bandgap

To further investigate the parameter effect of the honeycomb phononic crystal on bandgap, the thickness t of the plate and the radius r and the height h of the column are changed while the other parameters of the materials and the geometric structure are fixed. We choose the thickness t varying from 3 mm to 11 mm and the height h varying from 6 mm to 30 mm. Figure 13(a) shows that the width of the bandgap decreases as the thickness increases, and, when $t = 11$ mm, the bandgap disappears at the positions: $h = 6$ mm and $h = 30$ mm. We can easily find that the width of the bandgap is in a fluctuating state when the thickness t is kept unchanged and, at the height $h = 18$ mm, the width of bandgap reaches a maximum value. Figure 12(b) shows the effect of t and h on the lower edge of bandgap, and from this figure we can also see that the lower edge of bandgap reaches a minimum value when the height $h = 18$ mm with the thickness t are kept unchanged; of course, it does not include the case where there is no bandgap.

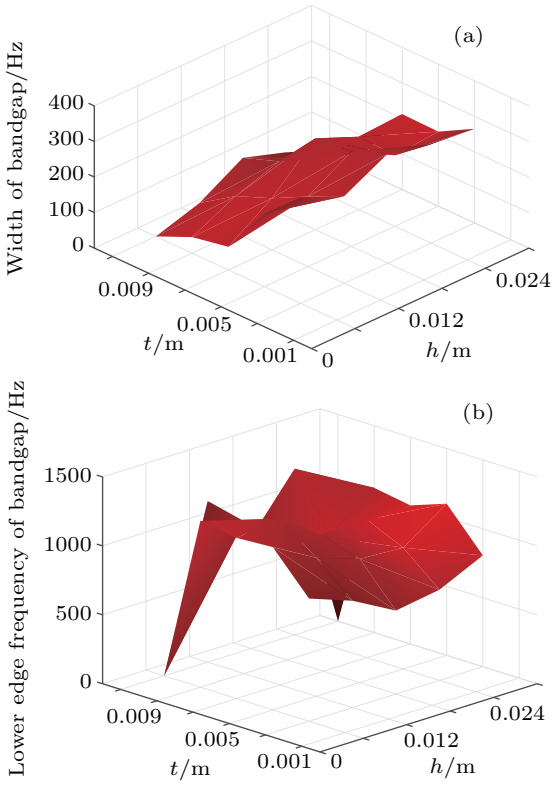


Fig. 13. (color online) Effect of t and h on (a) bandgap width and (b) low edge of bandgap.

From what has been discussed above, if we need to achieve a low frequency and wider bandgap of a honeycomb phononic crystal, we should reduce the plate thickness properly and find the best column height.

We study the effect of radius of the column on bandgap in this section. The thickness t is kept at 3 mm and the height h is kept at 18 mm. We change the radius r of the column from 3 mm to 10 mm, the first bandgap is between the 13th frequency and the 14th frequency. We can find from Fig. 14 that when the radius r increases, the 13th frequency has little change and just wanders around 600 Hz, while the 14th frequency has huge fluctuations, and the maximum value rises by up to 900 Hz when the radius $r = 8$ mm. The result shows that the column radius has little effect on the lower edge of the bandgap, while it has a huge effect on the upper edge. So, we can widen the bandgap as long as we choose an appropriate column radius.

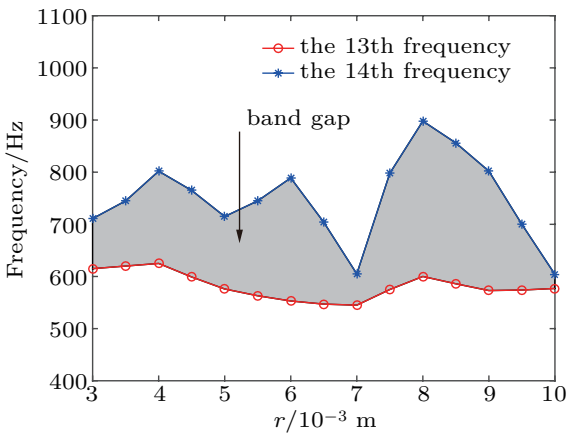


Fig. 14. (color online) Effect of column radius on bandgap.

6. Conclusions

In this paper, we have designed a honeycomb phononic crystal and calculated its bandgap by the FEM by noting that it has good vibration reduction performance in a frequency range of 600 Hz–900 Hz. We also analyze its vibration modes and transmission characteristic, which fits well to the bandgap. The simulation and corresponding experiment are also performed. The simulation results of the frequency response function of the system show that the honeycomb phononic crystal could reduce the vibrating plate magnitudes by up to 60 dB (averaging 21.03 dB), while the rubber plate can decrease it only about 20 dB. However, the experimental results (averaging 23.12 dB) are slightly larger than simulation results. The main reason for this is that the effect of damping in the simulation is not taken into consideration and there are some losses of energy in the experiment. In spite of this, the experimental results have the same trend as the simulation results in a frequency range of 600 Hz–900 Hz. It can further be

verified that this honeycomb phononic crystal has a perfect vibration reduction performance in its bandgap, which can have profound meaning for vibration reduction in practical applications. We also study the parameter effect on bandgap, and the results show that the width of the bandgap decreases with the thickness increasing and at the height $h = 18$ mm, the width of bandgap reaches a maximum value, with the thickness kept unchanged. In addition, we also find that the 13th frequency has little change and just wanders around 600 Hz while the 14th frequency fluctuates a lot as the radius increases. So, choosing the parameter appropriately can help us achieve a lower frequency and wider bandgap.

References

[1] Liang C H, Sun M X and Liu H X 2014 *J. Aerosp. Power* **29** 1701
[2] Zhang A, Cui L and Zhang P 2013 *IEEE Computer Society International Conference on Information Technology and Applications*, p. 462
[3] Chen G K, Wang Y and Zhang Y 2011 *IEEE International Conference on Industrial Engineering and Engineering Management*, p. 1760
[4] Jiang C, Deng M and Tomono T 2010 *IEEE International Symposium on Intelligent Control*, p. 2397
[5] Chen Y, Shi K and Wen X 2011 *Information and Management Engineering* (Berlin, Heidelberg: Springer) p. 66
[6] Tourajizadeh H and Zare S 2016 *Aerosp. Sci. Technol.* **50** 1
[7] Prakash S, Kumar T G R, Raja S, *et al.* 2016 *J. Sound Vib.* **361** 32
[8] Nutan R A and Raghavan S 2013 *IEEE International Conference on Emerging Trends in Computing, Communication and Nanotechnology*, p. 625
[9] Kushwaha M S, Halevi P, Martínez G, *et al.* 1994 *Phys. Rev. B* **49** 2313
[10] Liu Z, Chan C T and Sheng P 2005 *Phys. Rev. B* **71** 014103
[11] Sigalas M M and Economou E N 1992 *J. Sound Vib.* **158** 377
[12] Brillouin L 1953 *Wave Propagation in Periodic Structures*, 2nd edn. (New York: Dover Publications)
[13] Wen X S, Wen J H, Yu D L, *et al.* 2009 *Phononic crystals* (Beijing: National Defense Industry Press) ISBN: 9787118063424
[14] Tanaka Y and Tamura S I 1998 *Phys. Rev. B* **58** 7958
[15] Kushwaha M S and Halevi P 1997 *J. Acoust. Soc. Am.* **101** 619
[16] Liu Z M 2005 *National University of Defense Technology*
[17] Sigalas M and Economou E N 1993 *J. Solid State Commun.* **86** 141
[18] Liu Z Y, Zhang X X, Mao Y W, *et al.* 2000 *Science* **289** 1734
[19] Zhang Z and Han X K 2016 *Phys. Lett. A* **380** 3766
[20] Li F, Zhang C and Liu C 2017 *J. Sound Vib.* **393** 14
[21] Sun L 2017 *Appl. Acoust.* **119** 101